Particle Accelerators, 1994, Vol. 43(3), pp. 145–158
Reprints available directly from the publisher
Photocopying permitted by license only

LOW-ENERGY H^- INJECTOR DESIGN FOR SSC RFQ

CHUN FAI CHAN and KA-NGO LEUNG

Lawrence Berkeley Laboratory, University of California, Berkeley, CA 94720, USA

(Received 12 March 1993; in final form 19 August 1993)

An rf driven H^- source has been developed at Lawrence Berkeley Laboratory (LBL) for use in the Superconducting Super Collider (SSC). To date, an H^- current of ~40 mA can be obtained from a 5.6-mm-diam aperture with the source operated at a pressure of about 12 mTorr and 50 kW of rf power, with a pulse length of less than 1 ms. In order to match the accelerated H^- beam into the SSC radiofrequency quadrupole (RFQ), a low-energy H^- injection system has been designed. This injector produces an outgoing H^- beam of 30 mA at 35 keV, free of electron contamination, with a small radius, large convergence angle, and small projectional emittance.

KEY WORDS: Injectors, Ion Sources, Low Energy H^- Injector, Proton, SSC RFQ

1 INTRODUCTION

The negative ion of hydrogen is commonly used in the injector for modern circular proton accelerators since the invention of an ingenious injection scheme by Dimov and Budker.[1,2] In this paper we report a recently developed, rf-driven H^- "volume" source and a compact, flexible, low-energy injector for the stated purpose.

The advantage of an RF induction discharge as the ion source is that it can operate reliably and has a long life time, when compared with the usual discharge driven by filament cathodes. For a volume source, the H^- ions are cold, with an ion temperature of about 1 eV. This contrasts with those produced by a cesiated surface.[2] Thus it enables one to extract a beam with low emittance. This source development will be discussed in Section 2 below.

The extraction of H^- ions is accompanied by a large amount of electrons from the source, which must be removed before further acceleration. The remaining H^- ion beam must be focused properly to match the acceptance of the next element of the accelerator system, e.g., a radio-frequency quadrupole (RFQ). During this process, one must be careful with the ion beam optics so that the emittance growth can be kept as low as possible. In Section 3, one such injector design for the SSC RFQ is presented that meets the stringent requirements for matching parameters. Obviously a beam with the lowest possible emittance will give the maximum possible luminosity at the intersection regions of the collider. An optimally performing, low-energy injector is a good start and will contribute to this overall goal.

The specific example presented is for the requirement of the injector for the SSC RFQ. However, the design principles and method used here should be easily adaptable for injectors with similar requirements for other purposes.

2 THE RF-DRIVEN MULTICUSP SOURCE

2.1 Description of the Source

Multicusp plasma generators have been operated successfully as volume-production H^- sources.[3,4] The H^- ions formed by volume-production processes have low beam emittance and are therefore useful for the generation of high-brightness beams. In order to achieve high current densities, volume H^- sources require high discharge power. For this reason, the lifetime of the filament cathodes is normally short for steady-state or high-repetition pulsed operations. The use of an RF induction discharge as an H^- source is attractive for high-energy accelerator applications. There are no short-lived components in the source chamber. A clean plasma, free of contamination from the cathode material, can be maintained and the rf power supplies operate conveniently at ground potential.

At Lawrence Berkeley Laboratory (LBL), an RF-driven source has been operated successfully for the extraction of H^- beams.[5] In the past two years, we have optimized the filter and the collar geometry to obtain higher H^- output and lower electron current in the extracted beam. A schematic diagram of the RF ion source is shown in Fig. 1. The source chamber is a copper cylinder (10 cm diameter by 10 cm long) surrounded by 20 columns of samarium-cobalt (SmCo) magnets that form a longitudinal line-cusp configuration. The magnets are enclosed by an anodized aluminum cylinder with cooling water circulating between the magnets and the inner housing. The back flange has four rows of magnets cooled by water passages drilled in the copper.

In order to enhance the H^- yield, a pair of water-cooled permanent magnet filter rods is installed near the extraction region. The filter rods provide a narrow region of transverse magnetic field which divides the entire source chamber into a discharge and extraction region. The filter field is strong enough to prevent energetic electrons from reaching the extraction chamber. Excitation and ionization of the gas molecules take place in the discharge chamber. Positive and negative ions, together with cold electrons, are present in the extraction region. They form a plasma with a lower electron temperature,[6] which makes a favorable environment for the formation of H^- ions by dissociative attachment and their survival to reach the accelerator.

The plasma is generated by inductive discharge via a two-turn copper antenna. The RF antenna is fabricated from 4.7-mm-diameter copper tubing and is coated with a thin layer of hard porcelain material, which is slightly flexible and resistant to cracking. It has maintained a clean plasma in pulsed operation for periods of several weeks; however, the antenna life expectancy has not yet been determined.

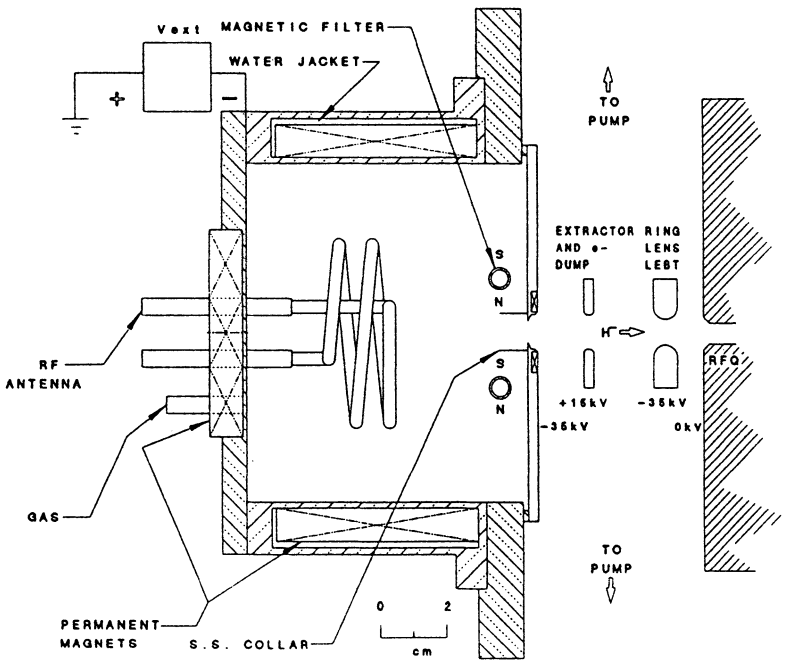

FIGURE 1: A schematic diagram of the RF multicusp source.

The antenna is connected to a matching network and isolation transformer, matching the 50-ohm impedance of the amplifier with the impedance of the plasma. The RF signal is generated by a digital synthesizer. The signal (~2 MHz) is sent to a preamplifier, and then to the rf amplifier. Peak performance allows a maximum pulsed RF input power of 50 kW. This power travels through a 50-ohm coaxial cable to the isolation and matching network. The RF power can be controlled by changing the amplitude and frequency of the synthesizer signal. Maximum efficiency is achieved when the output voltage and current from the RF amplifier are in phase and operating at a 50-ohm impedance. For pulsed operation, a small, hairpin tungsten filament is normally used as a starter for the RF induction discharge.

2.2 *Experimental Results*

Operation of the RF-driven, multicusp H^- ion source has been previously reported.[3,4] During the last two years, we have optimized the filter and the collar geometry to obtain higher H^- output and lower electron current in the extracted beam. Fig. 2

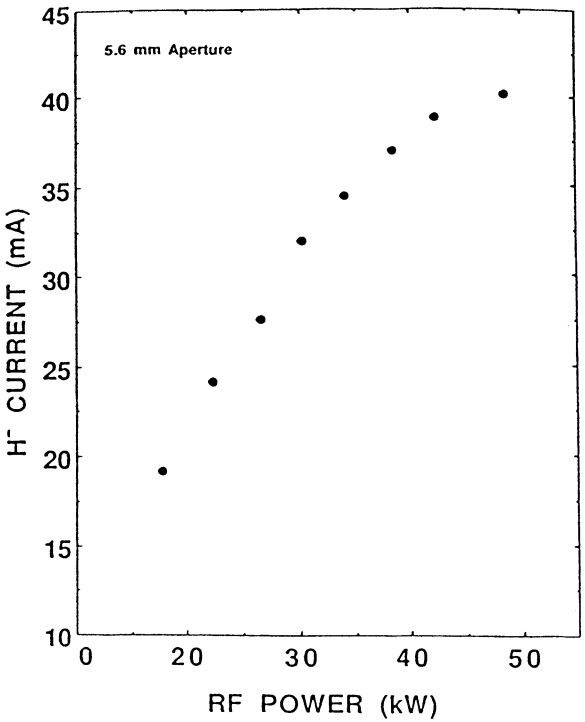

FIGURE 2: Extracted H^- current vs. RF power.

is a plot of the extracted H^- current as a function of RF input power. An H^- current of ~40 mA can be obtained from a 5.6-mm-diameter aperture with the source operating at a pressure of about 12 mTorr and 50 kW of RF power. The ratio of electrons to H^- ions in the extracted beam varies from 8 to 12 as the RF power is changed from 20 to 50 kW. Based on these experimental results, along with the previous emittance measurement[7,8] that shows an ion temperature of 1.5 eV, we have designed a simple four-electrode electrostatic injector system for the SSC RFQ.

3 LOW-ENERGY INJECTOR DESIGN

In this section we describe the design of an injector that would couple with the RF source and would deliver a useful H^- beam with desirable matching parameters to the RFQ. In the specific example provided, the exiting H^- beam of 30 mA at 35 kV has to meet the following requirements[9] in order to match the Twiss parameters for the SSC RFQ: beam radius = 0.2 cm, convergence angle = 139 mrad, and ε(rms) = 0.018 π·cm·mrad. The injector consists of four electrodes and is operated in an accel-

decel-accel scheme similar to a previous injector design.[10] The first two electrodes employ an acceleration voltage of 50 kV to extract the negative ions and the unwanted electrons. The latter are swept away by a pair of permanent magnets embedded in the first electrode. (The reason to choose the 50 kV value is to provide enough gap spacing for those deflected electrons to reach the second electrode.) The H^- beam is then decelerated by the third electrode (normally biased at the same voltage as the first one). The beam expands as it slows down. It is then reaccelerated and compressed by the fourth electrode, which is also the entrance to the RFQ. Several important improvements have been made over the preliminary version reported earlier.[11] They are described in the subsections below. Further improvements and extensions of the design are discussed in Section 4.

3.1 Special Techniques used in the Design Computation

We use an axisymmetric, 2-D, ion-beam optics code to compute the charged particle trajectories. In order to be precise, we include the effect of the attenuation of the H^- current due to gas stripping by modifying the current density along the z axis with the function f_i, shown in Fig. 3. Based on the geometry of the electrode structure, we performed a Monte Carlo code calculation to simulate the molecular flow and pumping,[11] once the gas pressure in the source is given. (We assumed a pumping speed of 2800 liter/second, the capacity of one large turbomolecular pump.) Then we were able to determine the pressure drop along the beam axis. For example, the pressure is reduced by a factor of 0.26 at 1 cm from the aperture, and 0.01 at 5 cm. The calculation of the beam survival fraction is based on the stripping cross-section of H^- with the gas molecules, which depends on the energy of the beam along its path. The function f_i is a fit to this numerical result. For a gas pressure of 12 mTorr, the survival fraction is about 92% at 5 cm.

For the extracted electrons, a method has to be devised to simulate their space-charge effect, at least in the direction of the symmetry axis. We use the function f_e shown in Fig. 3. It accounts for the full effect near the source aperture and is gradually turned off about 1 cm away.

In order to compute the rms projectional emittance, it is necessary to use the version of the code with "skew beam dynamics" described in Ref. 12. In this code, each beamlet is launched with axial, radial, and azimuthal velocities.

3.2 Design Goals and Results

The specific goals mentioned above are fulfilled with the design shown in Fig. 4. An H^- current density of $j_o = 115$ mA/cm^2 and an electron-to-ion current ratio of 11 to 1 are assumed at the source aperture, which has a radius $r = 0.3$ cm. As the beam travels about 5 cm to the exit, it retains about 92% of its current according to the function f_i shown in Fig. 3. We also assume a uniform current-density distribution at the aperture and an ion temperature $kT_i = 1.5$ eV. Thus the initial rms emittance is

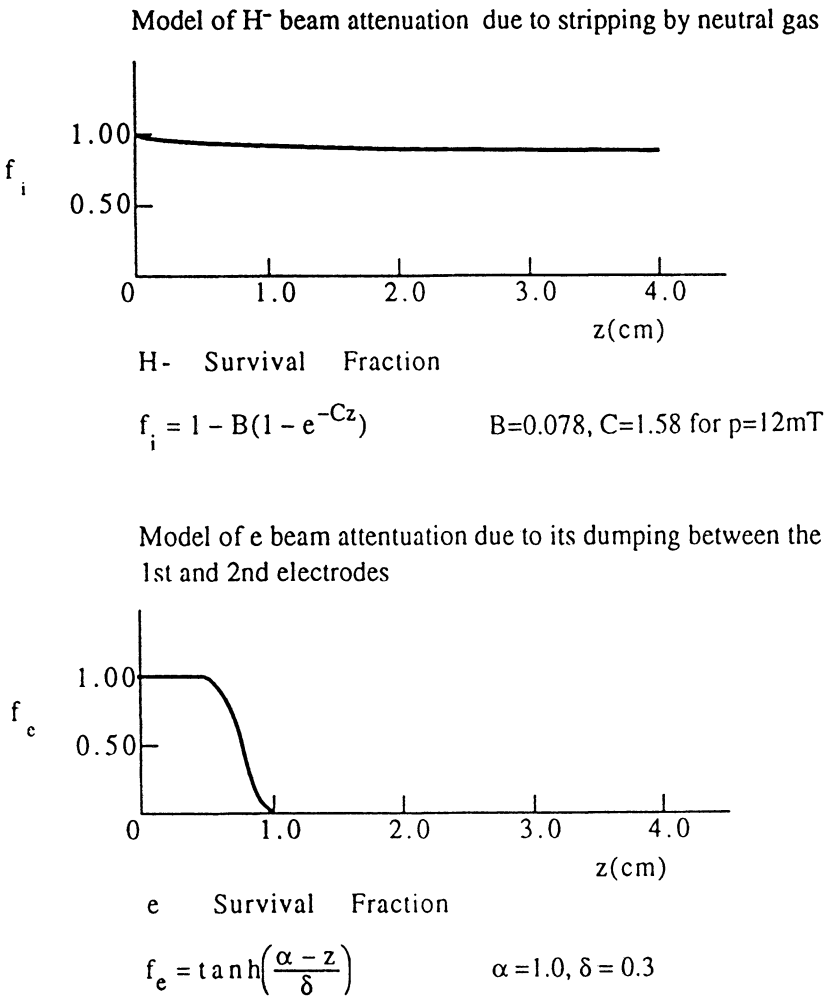

FIGURE 3: Models of beam attenuation profiles.

0.006 π·cm·mrad at that location.[13] The $x - x'$ phase plot in Fig. 4 shows 90% of the emittance as the beam enters the last electrode. The length of the first gap is chosen in such a way that it nearly saturates to the Child-Langmuir limit with an acceleration voltage of 50 kV. The shape of the first electrode is optimized to ensure a flat plasma emission surface, which is defined by the once-integrated Poisson equation,

$$\frac{v_z}{v_o} = 1 + 3.06 \times 10^{-2} \frac{E^2}{m^{1/2}(kT_i)^{1/2} j_o}, \tag{1}$$

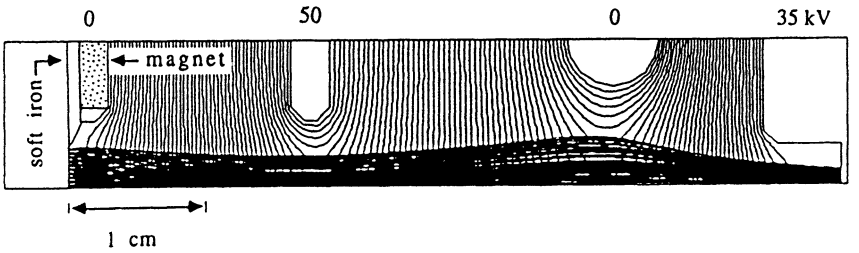

Extraction aperture radius = 0.3 cm

I_{H^-} = 30 mA at exit

ε_{1rms}= 0.009 π-cm-mrad at exit

j_e/j_{H^-} = 11/1 at the source aperture

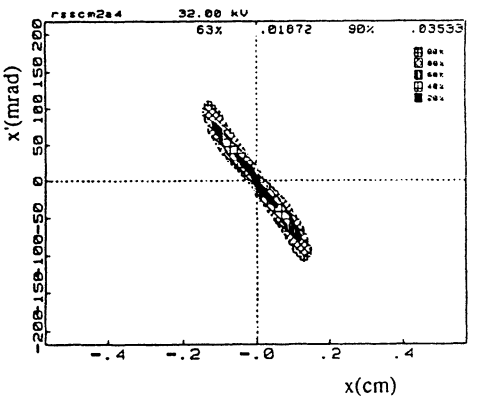

FIGURE 4: Axisymmetric beam trajectory plot and exit phase space diagram.

where $v_o = (2kT_i/m)^{1/2}$ is the thermal velocity of the ion, j_o is the initial current density in A/cm^2, m is the mass of the ion in amu, and E is the electric field in kV/cm. From this relation, the initial axial velocity of the beam v_z is calculated. A self-consistent emitter is achieved if the normal electric field, calculated by the beam optic code, agrees with the input E. (In this case the input E is set at a relatively low value of 1 kV/cm.)

The voltages of the four electrodes are 0, 50, 0, and 35 kV, respectively. Alternatively, they can be labelled as –35, 15, –35 and 0 kV, because these voltages would produce the same result.

Fig. 5 shows the calculated growth of the rms emittance as the beam propagates. Care must be taken when we expand and compress the beam in order to get a large convergence angle into the RFQ. Otherwise one would produce a highly nonlinear shape in phase space, with large rms emittance.

The potential of the third electrode is normally equal to that of the first electrode. However, if a larger convergence angle of the beam into the RFQ is desired, it should be biased at a few kV negative with respect to the first electrode. With this, one can adjust the beam angle continuously to provide the proper entrance angle for a particular RFQ requirement. An example is shown in Fig. 6.

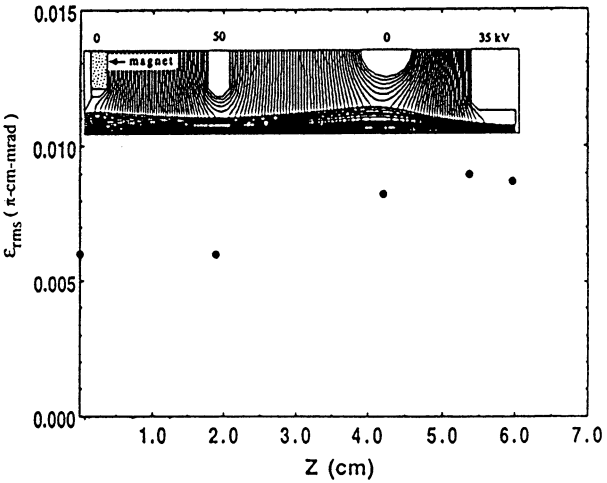

FIGURE 5: Emittance growth along the beam path.

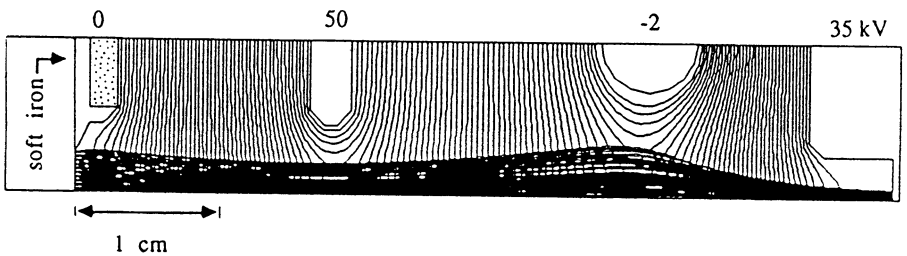

Extraction aperture radius = 0.3 cm

I_{H^-} = 30 mA at exit

ε_{1rms}= 0.010 π-cm-mrad at exit

j_e/j_{H^-} = 11/1 at the source aperture

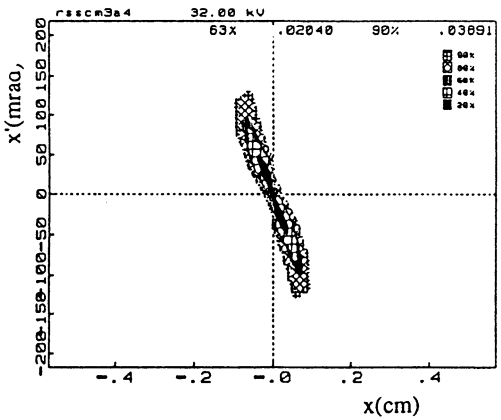

FIGURE 6: Axisymmetric beam trajectory plot and exit phase space with a larger convergence angle.

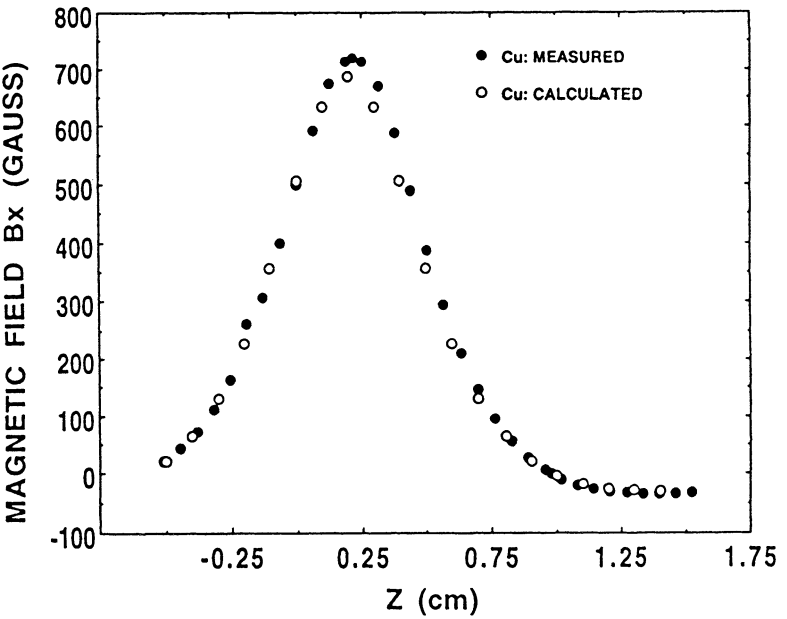

FIGURE 7: Comparison of the axial B fields produced by a pair of SmCo magnets: calculated and measured, both with copper housing.

In these results (Figs. 4–6) we have eliminated an intermediate electrode between the present second and third electrodes. The arrangement of the electrodes of the present design is simpler and more open, and therefore allows better gas pumping. It is also a further departure from the orthodox einzel-lens approach.[14]

3.3 Dumping of the Electrons

One of the problems of extracting negative ions from a volume source is that the beam contains a large amount of unwanted electrons. Putting a pair of permanent magnets (e.g., SmCo) inside the first electrode can sweep those electrons out of the beam at the early stage of acceleration. However, a closer examination of this solution[11] reveals that the magnets of proper size and strength to achieve this result would also produce a **B** field of about 500 gauss at the source aperture (at z=0.0), extending and gradually diminishing into the source chamber. Fig. 7 shows the calculated and measured **B** field as a function of axial position. This penetration would have a destructive effect on the H^- production there.

A method was found to solve this problem. For the first electrode, we replaced the usual copper material with soft iron. The locations of the SmCo magnets are shown in

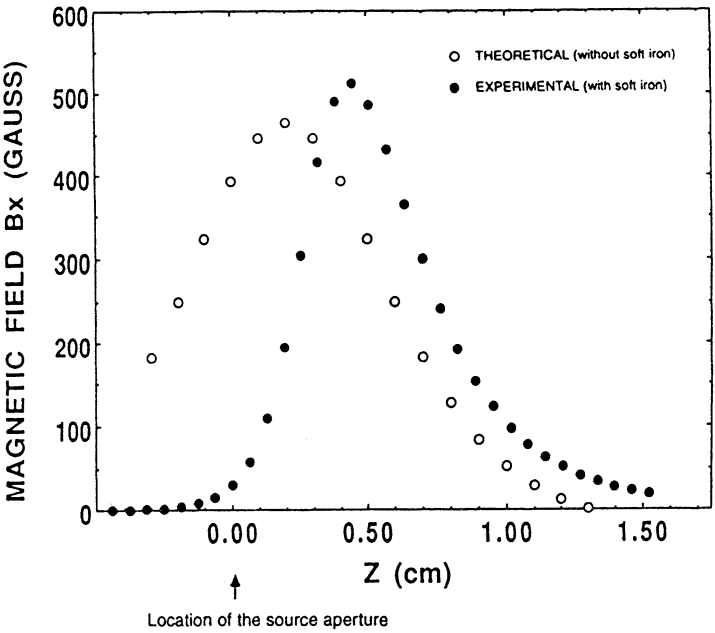

FIGURE 8: Comparison of the axial B fields produced by a pair of SmCo magnets: calculated (corresponding to copper housing) and measured (with soft iron housing). Note: the magnet goemetry is slightly different from that in Fig. 7.

Fig. 4 and Fig. 6. This soft iron housing has the effect of shifting the peak of the **B** field away from the source and greatly reduces the penetration, as shown in Fig. 8. A detailed preliminary version of the hardware arrangement for this electrode is shown in Fig. 9. (For ease of fabrication, it does not have the exact dimensions and shape of the first electrode shown in Fig. 4. However, it does demonstrate the effect of the soft iron housing.)

In Fig. 10 we simulate this shifted **B** field in a planar calculation to study the trajectories of the electrons. The exact landing location of the electrons on the second electrode is not critical as long as they are stopped from going further downstream. Since the present design is for short-pulse operation (less than 1 ms.) and low duty factor, the heat loading should not pose a problem, especially if active cooling is employed.

There is one further advantage of this accel-decel injector design. There exists an electric field reversal before and after the second electrode. Any secondary emission of electrons produced by the impact of the extracted source electrons on the upstream face of the second electrode would be confined to the first gap and would not migrate

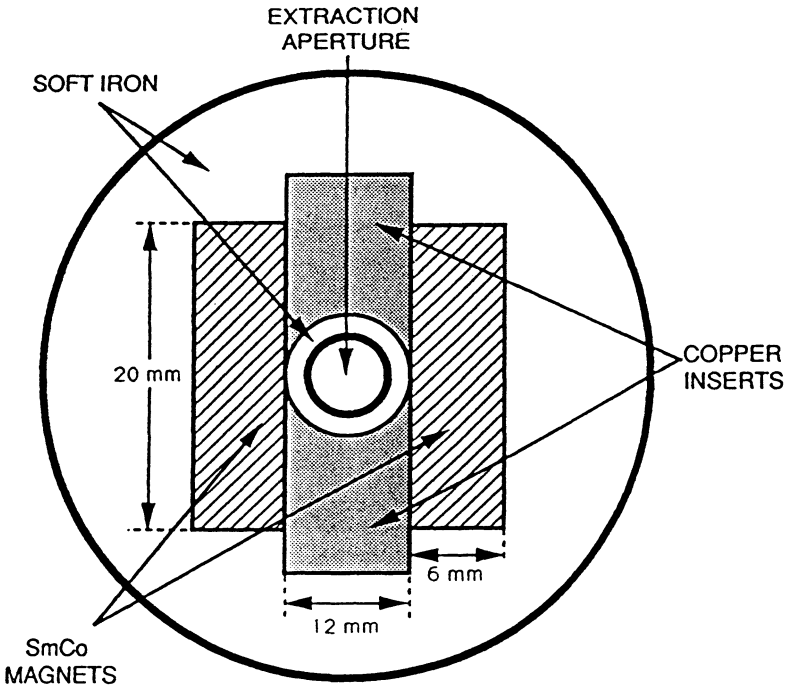

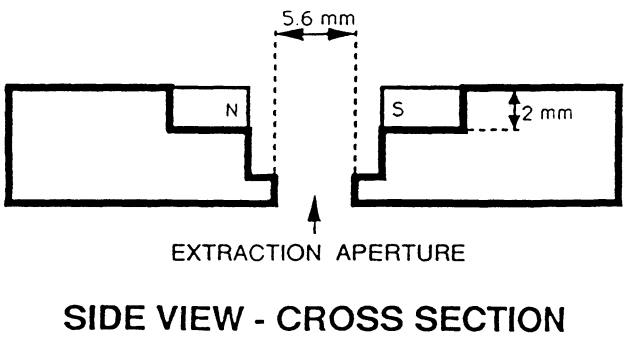

FIGURE 9: Detail of preliminary extraction electrode that produced the shifted magnetic field shown in Fig. 8.

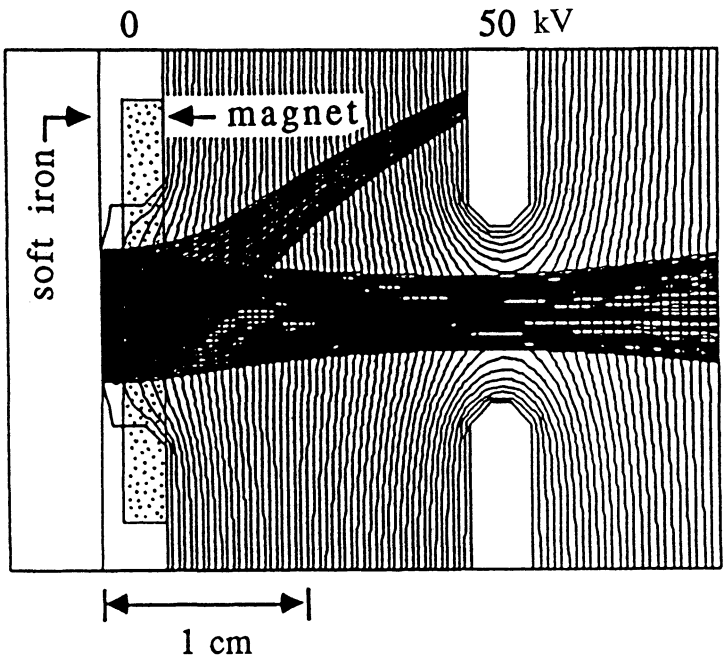

FIGURE 10: Planar calculation showing the effect on the extracted electrons due to a pair of magnets located inside the 1st electrode.

downstream to cause damage or to produce x rays. Furthermore, the fast acceleration of the ions and electrons after the source aperture can minimize the effect of their mutual repulsion due to space charge once the electrons are deflected aside by the magnetic field. In the planar calculation (Fig. 10), it is shown that this repulsive force on the ions partially compensates the deflecting magnetic force. The phase plot (not shown) at the exit of the second electrode indicates a slight displacement of the emittance as a whole, with no noticeable nonlinear distortion.

4 DISCUSSIONS AND CONCLUSIONS

We have described in Sections 2 and 3 an RF-driven H^- volume source and the design of a compact low-energy injector to produce an H^- beam with large convergence angle and low emittance. The overall arrangement is shown in Fig. 1. The calculated exit emittance is about a factor of two smaller than the SSC RFQ injector requirement. This is achieved by good ion beam optics and the low H^- ion temperature produced by the volume source. In this study, we have ignored the contribution of the emittance growth due to the perturbation of the ion trajectories by the magnetic field, as well

as its steering effect on the beam as a whole. However, we don't expect these effects to be dominant factors. This assertion is partially supported by the planar calculation mentioned above. Experimentally,[8] we found that for a similar source with a radius of 0.5 cm for the extraction aperture and with a similar electron/H^- ion separation system, the observed final rms emittance is 0.0095 π·cm·mrad. This result is consistent with our calculated final rms emittances shown in Figs. 4–6. We intend to investigate this issue in more detail with 3-D calculations in the future.

The question of how to dump the electrons without much interference with the performance of the source is a longstanding problem for H^- ion extraction. We believe that we have found a simple method, described in Subsection 3.3, to provide decoupling to resolve this issue. The modification of the present design to accommodate dc operation is under study and shall be reported elsewhere.

ACKNOWLEDGMENTS

We thank Russell Wells for the gas flow and beam stripping calculation and William Steele for the emittance contour plotting program. This work is supported by the Office of Energy Research, Office of Superconducting Super Colllider via the Superconducting Super Collider Laboratory, and by the Office of Energy Research, Office of Fusion Energy, Development and Technology Division of the U.S. Department of Energy under Contract No. DE-AC03-76SF00098.

REFERENCES

1.. G.I. Dimov and G.I. Budker, international conference (1963), CONF-114, U.S. Atomic Energy Commission publication TID-4500, p. 1372.

2.. K.W. Ehlers, invited talk, in *Proceedings of the 15th International Conference on Ion Sources* (Berkeley, CA, 1989), Rev. Sci. Instrum., **61** (January 1990) 1. In this review talk, other applications of H^- beams are also discussed.

3.. K.N. Leung, G.J. DeVries, W.F. DiVergilio, R.W. Hamm, C.A. Hauck, W B. Kunkel, D.S. McDonald, and M.D. Williams, Rev. Sci. Instrum. **62** (1991) 100.

4.. K.N. Leung, W.F. DiVergilio, C.A. Hauck, W.B. Kunkel, and D.S. McDonald, in *Proceedings of the 1991 IEEE Particle Accelerator Conference* **3**, p. 1919, (San Francisco, CA, 1991).

5.. K.N. Leung, D.A. Bachman, C.F. Chan, and D.S. McDonald, in *Proceedings of the Conference on High Energy Accelerators* HEACC'92 (Hamburg Germany, 1992), Int. J. Mod. Phys. A (Proc. Suppl.) **2** (1993) p. 200; J. Rossbach, ed.

6.. K.N. Leung, K.W. Ehlers, and M. Bacal, Rev. Sci. Instrum., **54** (1983) 56.

7.. G. Gammel, T. Debiak, J. Sredniawski, K. N. Leung, and D. McDonald, in *Proceedings of 1991 Particle Accelerator Conference* **4**, p. 2023, (San Francisco, CA, 1991).

8.. J.W. Kwan, G.D. Ackerman, O.A. Anderson, C.F. Chan, W.S. Cooper, G.J. deVries, W.B. Kunkel, K.N. Leung, P. Purgalis, W.F. Steele, and R.P. Wells, Rev. Sci. Instrum. **62**,(6) (1991) p. 1521. This paper reported the experimental result of the preaccelerator whose design was presented in Reference 10.

9.. Warren Funk, private communication (May 1991).

10.. C.F. Chan and A.F. Lietzke, Bull. Am. Phys. Soc. **34**, 9, (1989) p. 2116.

11.. O.A. Anderson, C.F. Chan, K.N. Leung, L. Soroka, and R.P. Wells, Rev. Sci. Instrum. **63**, 4, (1992) p. 2738.

12.. C.F. Chan, W.S. Cooper, J.W. Kwan, and W.F. Steele, Nucl. Instrum. Meth. **306**, (1991) p. 112.

13.. See, for example, J.D. Lawson, *The Physics of Charged-Particle Beams*, 2nd edition (Oxford University Press, New York, 1988), (1988) p. 210.

14.. See, for example, *Applied Charged Particle Optics*, Part A, edited by A. Septier (Academic Press, New York, 1980), p. 314; Advances in Electronics and Electron Physics, edited by P.W. Hawkes, **76** (1989), pp. 5, 107; P.W. Hawkes and E. Kasper, *Principles of Electron Optics* (Academic Press, London and San Diego, 1989), p. 678; I. Brown, *The Physics and Technology of Ion Sources*, edited by Ian G. Brown (Wiley, New York, 1989), p. 61; and O. A. Anderson *et al.*, in Proceedings of 2nd European Particle Accelerator Conference (Nice, France, 1990), p. 1288.